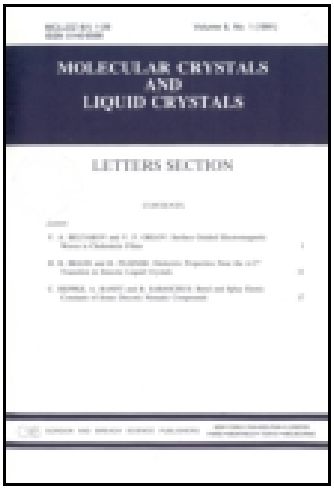

Molecular Crystals and Liquid Crystals
Publication details, including instructions for authors and subscription information:
http://www.tandfonline.com/loi/gmcl20

Poly(N-vinylcarbazole) Film-Based Liquid Crystal Films

Andy Ying-Guey Fuh[abc], Yuan-Di Chen[a] & Ko-Ting Cheng[d]
[a] Department of Photonics, National Cheng Kung University, Tainan, Taiwan
[b] Department of Physics, National Cheng Kung University, Tainan, Taiwan
[c] Advanced Optoelectronic Technology Center, National Cheng Kung University, Tainan, Taiwan
[d] Department of Optics and Photonics, National Central University, Chung-Li City, Taiwan
Published online: 30 Sep 2014.

To cite this article: Andy Ying-Guey Fuh, Yuan-Di Chen & Ko-Ting Cheng (2014) Poly(N-vinylcarbazole) Film-Based Liquid Crystal Films, Molecular Crystals and Liquid Crystals, 596:1, 135-151, DOI: 10.1080/07315171.2014.918755

To link to this article: http://dx.doi.org/10.1080/07315171.2014.918755

Mol. Cryst. Liq. Cryst., Vol. 596: pp. 135–151, 2014

ISSN: 1542-1406 print/1563-5287 online
DOI: 10.1080/07315171.2014.918755

Taylor & Francis
Taylor & Francis Group

Poly(N-vinylcarbazole) Film-Based Liquid Crystal Films

ANDY YING-GUEY FUH,[1,2,3,*] YUAN-DI CHEN,[1] AND KO-TING CHENG[4]

[1]Department of Photonics, National Cheng Kung University, Tainan, Taiwan
[2]Department of Physics, National Cheng Kung University, Tainan, Taiwan
[3]Advanced Optoelectronic Technology Center, National Cheng Kung University, Tainan, Taiwan
[4]Department of Optics and Photonics, National Central University, Chung-Li City, Taiwan

The electro-optical properties of poly(n-vinylcarbazole) (PVK) film-based liquid crystal (LC) films are reported. Firstly, the alignment direction of a rubbed PVK film is found to successfully switch toward the rubbing direction through thermal treatment. Second, a method of particular thermally induced phase separation (TIPS) of LCs and polymers is presented. The method involves a combination of dissolution process and TIPS. Additionally, a scattering-mode light shutter having the advantages of low driving voltage, polarization-independent scattering, fast response, high contrast ratio is reported. Finally, the scattering-mode light shutter with different transmission is achieved by illuminating the cell under various light intensities.

Keywords Liquid crystal; PVK; phase separation; azo dyes; and scattering

1. Introduction

In recent decades, liquid crystals (LCs) have been widely developed for use in many optical devices, such as light shutters [1–2], switches [3], waveplates [4, 5], lenses [6], optical tweezers [7, 8], polarization rotators [9, 10], and so on. Among them, axially symmetric applications of LCs have received considerable attention owing to the great potential of LCs for use in electro-optical devices. Moreover, axially symmetric LC alignment, which is difficult to be fabricated, is suitable for the fabrication of the described electro-optical devices and for use in other applications. A linear polarization rotator can continuously change the direction of polarization of linearly polarized light according to the position of the incident beam onto the linear polarization rotator. Methods for fabricating a linear polarization rotator have been widely studied. They include two-direction rubbing [9] and photoalignment by azo dye-adsorption onto substrates [10]. Linear polarization rotators that are fabricated using the above two methods can rotate the direction of polarization of

*Address correspondence to Andy Ying-Guey Fuh, Department of Physics, Department of Photonics, Advanced Optoelectronic Technology Center, National Cheng Kung University, No. 1, University Road, Tainan City 70101, Taiwan. Tel.: +886-6-2757575x65228; Fax: +886-6-274-7995. E-mail: andyfuh@mail.ncku.edu.tw

incident linearly polarized light by between 0° and 90°. Also, scattering mode LC light shutters have been fabricated by phase transition/separation methods in polymer-dispersed LCs (PDLCs) [11–13], and polymer-stabilized cholesteric textures [1–3]. However, the polymer matrix walls produce a strong surface anchoring effect that increases driving voltages, indicating that the operated voltage of a traditional PDLC scattering mode light shutter is high, i.e. over 30 V [14, 15]. Accordingly, many scientists have recently paid much attention to reduce the operated voltage of PDLCs. Moreover, with regard to smart LC devices, optically addressed devices based on LCs have been extensively studied. In this study, we propose radial LC alignment layers, thermally-switched LC alignments, and particular thermally induced phase separation, using circular rubbing of poly(N-vinyl carbazole) (PVK) films, thermal treatment onto rubbed PVK films, and thermal treatment onto spin-coated PVK films, respectively. Additionally, we also demonstrate several applications of polarization rotators, optically and thermally controllable scattering mode light shutters, and others. All of them will be individually described in this paper.

About the key material of the study, that is PVK. As well known, many scientists worldwide have recently paid much attention to a photoconductive polymer material, PVK [16–20]. Golemme *et al*. reported high-resolution photorefractive PDLCs using PVK as a matrix to fabricate highly efficient gratings [18]. Huang *et al*. presented an electro- and photo-controllable spatial filter based on an LC film with a photoconductive layer of PVK [16–17]. Additionally, PVK materials have been demonstrated to improve the efficiency of light emitting diodes. Firstly, we reported that the mechanical rubbing of not only a PVK layer but also a polystyrene layer can induce a homogeneous alignment of LCs with their easy axes perpendicular to the rubbing direction [21]. The properties of LCs that aligned by rubbed PVK are similar to those of LCs that are aligned by rubbed polystyrene. The key to aligning LCs perpendicular to the rubbing direction is the anchoring that is induced by the phenyl rings in the side chain fragments of PVK and polystyrene. Hasegawa *et al.* reported that the position of phenyl rings in polystyrene determines the direction of alignment of LCs [22]. Accordingly, LCs are aligned along the phenyl rings by dipole-dipole interaction. Nakajima *et al.* also demonstrated that the unidirectional alignment of LCs provided by the polystyrene film can be changed toward the direction of rubbing by thermal treatment at various temperatures, because of the micro Brownian motion of the side and main chains [23]. However, the alignment direction of a rubbed PVK film has been found to successfully switch toward the rubbing direction through thermal treatment. The angle of re-orientation of the director axis increases with the temperature within a specific range. Thus, the current study concluded that the ability of LC alignment to be modified from twisted nematics to homogeneous alignment using thermal treatment [20]. The optical properties of linear and concentric polarization rotators, fabricated using a rubbed PVK film with thermal treatment, are examined.

In addition to radial alignment and thermally-switched LC alignment, a method of particular thermally induced phase separation (TIPS) of LCs and polymers is presented. The reported phase separation approach can be used to produce a rough PVK film that "realigns" LCs into multiple and micron-sized LC domains. The fabrication involves using disordered LC alignment based on thermally treated double-sided PVK films (no rubbing treatment). Two main mechanisms of scattering for such a light shutter exist, namely, surface scattering and volume scattering [24, 25]. Surface scattering is produced by the interface roughness between LC and the rough PVK surfaces, whereas volume scattering is caused by an inhomogeneous change in refractive index induced by the disordered LC alignment (multi-domains). The domain size generated determines the scattering performance [26, 27]. Moreover, the demonstrated electrically controllable LC light shutter in the scattering

mode has the advantages of low driving voltage, fast response, being polarizer free, and high contrast ratio, indicating its extremely promising potential applications. The electro-optical properties of the light shutter and the morphologies of the PVK layers are examined in detail.

Finally, this investigation also demonstrates scattering mode light shutters with different transmission (scattering) by light-induced dissolution of PVK based on DDLCs in a PVK films-coated LC cell. The stably multiple scattering performances, or the so-called multistable scattering modes, generated by reformed PVK layers with several domain sizes can be applied for achieving several scattering modes. Scattering is induced by the disordered LC distribution of optically treated double-sided PVK films. The light-induced dissolution of PVK based on DDLCs includes two main mechanisms, namely, the light-induced thermal effect and the photoisomerization effect [28–31]. The solubility of PVK in DDLCs directly depends on the temperature of the DDLCs and the population of the azo dye *cis*-isomers, resulting in low order parameter and reduction of clearing temperature. The temperature of the DDLCs results from the light-induced thermal effect, whereas the population of the *cis*-isomers is from the photoisomerization of azo dyes (DR1). These details of the light-induced dissolution and morphologies of the PVK layers are also examined. Additionally, the optically switched scattering state can be completely switched back to the original scattering state by treating with the particular TIPS process [32]. Restated, the stable scattering performance can be optically controlled, and the multistability of scattering light shutter can be successfully achieved. This multistable light scattering can be used for display devices and other potential applications.

2. Fabrication of PVK Films

The photoconductive polymer is PVK ($n_{\mathrm{PVK}} = 1.68$), purchased from Aldrich. The fabrication processes are different from those of conventional PDLCs cells. A solution of chlorobenzene solvent with PVK at a weight ratio of 98.36:1.64 was prepared to coat the PVK (powder) film onto indium-tin-oxide (ITO)-coated glass slides. The solution was then spin-coated onto the ITO-coated glass slides. The substrates were pre-baked in an oven at 80°C for 20 min, and post-baked at 120°C for 120 min after coating. The thickness of the fabricated PVK film, no mechanical rubbing, was measured to be of sub-micrometer ($\sim$0.2 μm) order using the Alpha-Step IQ Surface Profiler (KLA-Tencor). Moreover, two non-rubbed PVK-coated glass substrates were combined to fabricate an empty cell. Finally, the LC was homogeneously filled into the empty cell, and the edges of the cell were sealed with epoxy to produce a sample. The fabricated LC cell was transparent and very stable at room temperature ($\sim$25°C).

3. Results and Discussion

3.1 Thermally-Switched LC Alignment Based on Rubbed PVK Films [19, 20]

Refer to our previous study, we present a simple method to produce radial LC alignment layers using circular rubbing of PVK films. The produced layer can be used for fabricating axially symmetric homogeneous-radial, homeotropic-radial and radial-radial LC alignment devices by combing a rubbed PVK-coated substrate with another one with a desired LC alignment layer. A few materials, such as PVK, can be mechanically rubbed to induce

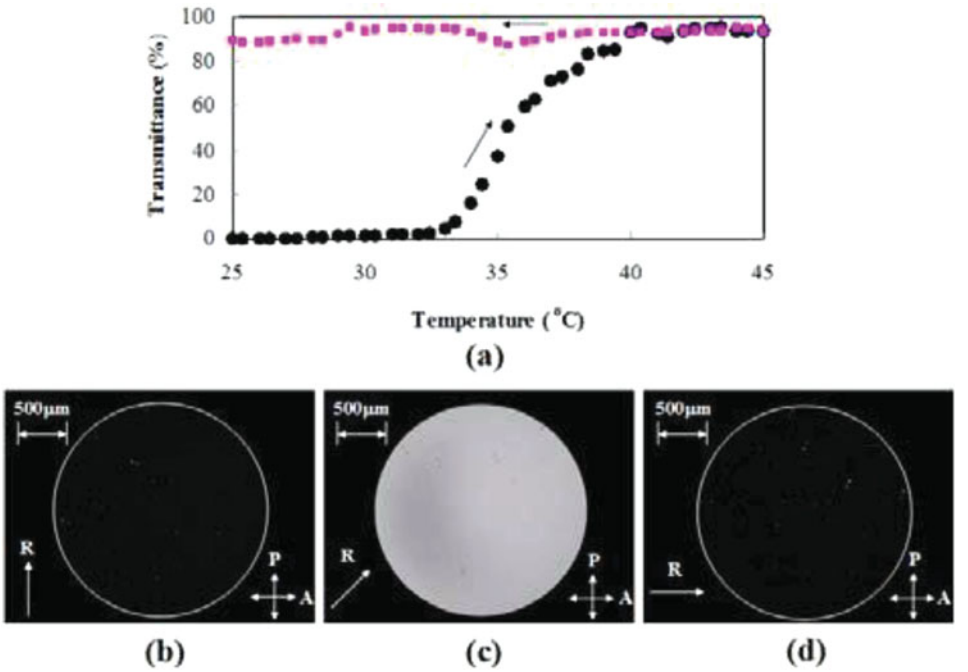

Figure 1. (a) Variations of stable transmittance with temperature of TN LC sample in heating and cooling. Images of LC sample observed under crossed-POM, after thermal treatment with **R** at an angle of (b) 0°, (c) 45° and (d) 90°, with respect to the transmission axis of the polarizer under a crossed-POM. **P** and **A** are transmission axes of polarizer and analyzer.

planar alignment of LCs with an easy axis that is perpendicular to the rubbing direction [21]. The investigation on PVK material for achieving a LC planar alignment was firstly demonstrated by Kaczmarek *et al* [21]. Such materials can be coated onto a substrate and treated with conventional circular rubbing to quickly form a radial LC alignment layer. In this section, it is reported that the thermally-switched LC alignment based on rubbed PVK films, and their application for polarization rotators. Initially, a twisted nematic (TN) cell was fabricated by two indium-tin-oxide (ITO)-coated glass slides; the inner surface of one of the slides was coated with an alignment film of poly(vinyl alcohol) (PVA), while the other was coated with a PVK film. Both films were rubbed in the direction, **R** (Fig. 1). The fabricated TN cell, filled with nematic LCs (E7) was then heated to study the thermally-switched LC alignment. Experimentally, thermal treatment reduced the twisted angle of the TN LC cell, and finally a TN aligned LC cell became a homogeneously aligned one. Concentric polarization rotators were demonstrated using this approach. The details of the fabrication process and the performance of the polarization rotators are presented below. It should be noted that the continually rotating range of the demonstrated polarization rotators can be varied if the LC material is properly selected. Additionally, pure PVK films cannot absorb the energy of visible light. Therefore, the polarization rotators can be operated in the broadband range of incident light, and have potential for the fabrication of phase modulators, spatial filters, LC lenses, and other optical elements because of the property of

electrically controllable birefringence. The LC phase modulators can perform both phase-only and amplitude modulations, depending on the polarizations of the incident beam [33]. Several reported LC lenses resulting from the spatial distribution of refractive indexes of the used LCs are polarization-dependent because the incident polarized light with various linear polarization experiences a different refractive index variation [34]. Additionally, several polarization-independent LC lenses have also been developed, based notably on polarization-dependent refractive index change [35, 36].

Figure 1(a) plots the variation with the temperature of the stable transmittance of the TN LC cell that was fabricated from the rubbed PVA and PVK substrates. Notably, the time required to reach stable transmittance was experimentally determined to depend on temperature. A lower temperature setting corresponds to a longer required duration. Initially, the TN LC sample was placed between two parallel polarizers that were in normally black mode, and the probe beam was normally incident onto SR. The transmission axes of the polarizers were set parallel to the rubbing direction. According to the experimental results, when the sample was heated, the transmittance initially remained almost unchanged, and then gradually increased with temperature above the threshold of $\sim$33°C. Finally, the transmittance ($\sim$0.95) saturated at temperature of $\sim$41°C, which was below the clearing temperature of the used LCs. The twisted angle decreases with the increase of temperature. This result can be easily understood since the LC alignment anchoring resulted from the rubbed PVK film before and after thermal treatments are orthogonal. The effective anchoring (torque) resulted from the combination of the side and main chains of the PVK film to align LCs toward the rubbing direction increases with the temperature. Accordingly, thermally-switched LC alignment anchoring to align LCs at angles from 90° to 0° with respect to **R** becomes stronger as temperature increases. Moreover, when the heated LC sample ($\sim$45°C) was cooled down to the room temperature, the stable transmittance remained almost unchanged. Therefore, the thermally-switched LC alignment is irreversible. Accordingly, the thermally-switched LC alignment layer is definitely stable. Figures 1(b)–1(d) show images of the LC sample after thermal treatment (heating to $\sim$45°C followed by cooling to room temperature) when the rubbing direction (**R**) was at 0°, 45° and 90°, respectively, to the transmission axis of the polarizer in a crossed-polarized optical microscope (POM). Clearly, the absence (presence) of the phase retardation ($2\pi d\Delta n/\lambda$) in Figs. 1(b) and 1(d) [1(c)] was responsible for the dark (bright) state. Hence, the thermally-switched LC alignment anchoring is inferred to have been caused by the rubbed PVK film after thermal treatment changes the LC alignment from TN to homogeneous alignment. Such an alignment film is highly uniform. According to the properties of thermally-switched LC alignment that was based on rubbed PVK film, and concentric polarization rotators were successfully demonstrated using a thermal gradient.

A concentric polarization rotator was fabricated using the experimental setup that is shown in Fig. 2(a). A solid copper cone was utilized as a medium to transmit heat from the hot plate to the TN LC cell that was fabricated by combining substrates with rubbed PVA and PVK films. The diameters of the upper and lower contact areas of the solid copper cone were 1 and 11 mm, respectively. The temperature of the hot plate was set to $\sim$45°C to heat the LC sample for 1 minute. Afterwards, the sample was cooled naturally to room temperature. The thermal diffusion in the area in contact with the upper cone established a radial thermal gradient. Figure 2(b) depicts the top-view LC configuration in the concentric polarization rotator. The LC alignment of the central region was homogeneous, and the region that was far from the heated cone remained in the 90° TN state.

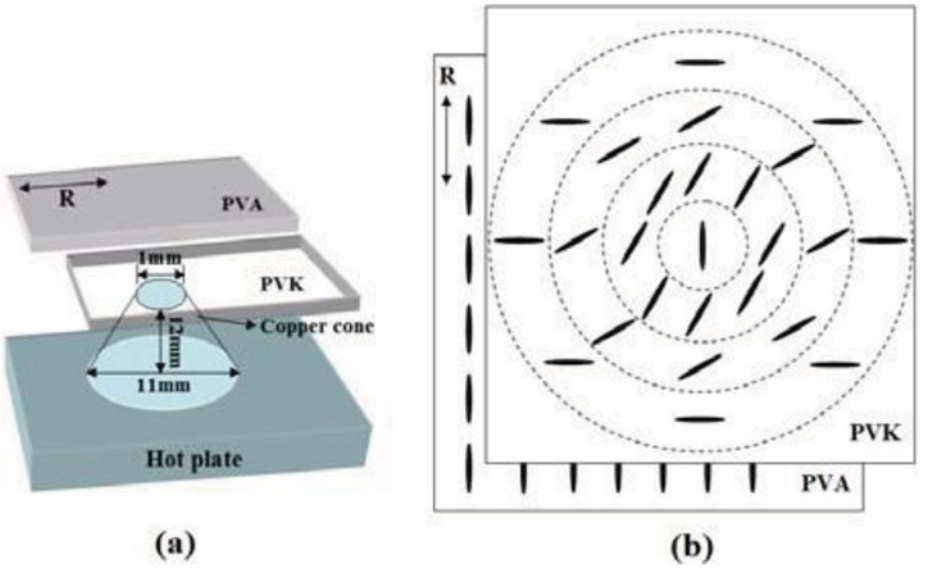

Figure 2. (a) Experimental setup for fabricating concentric polarization rotator; (b) LC directors in a concentric polarization rotator.

Figures 3(a)–3(d) present photographs of the fabricated concentric polarization rotator observed under two polarizers in which **P** was parallel with **R**, and **A** was set at 0°, 45°, 90° and 135° with respect to **R**, respectively. Clearly, the continually rotating angles of the concentric polarization rotator change from 0° (center) to 90° (margin). Also, the transmittances of the formed concentric polarization rotator were measured at various positions to determine the range of continuous rotation. Figures 3(e) and 3(f) plot the transmittance

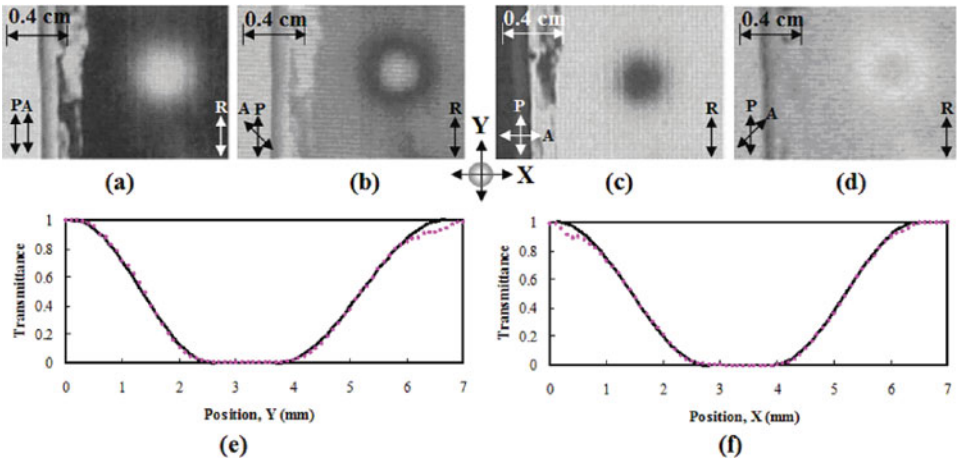

Figure 3. Photographs of fabricated concentric polarization rotator observed under two polarizers, with **P** parallel to **R** and **A** set to an angle of (a) 0°, (b) 45°, (c) 90° and (d) 135° with respect to **R**. Transmittance of concentric polarization rotator as a function of laser beam position along (e) **X** and (f) **Y** directions. Dotted and solid lines plot experimental and theoretical results, respectively.

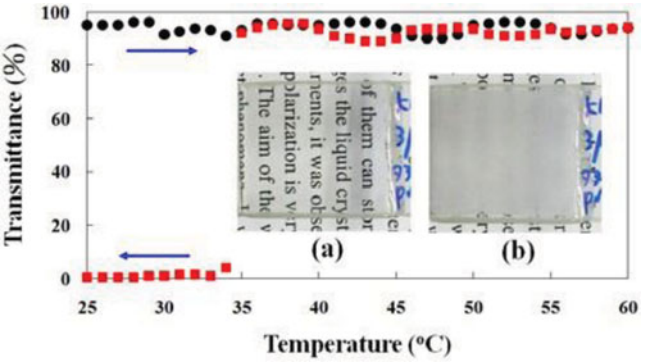

Figure 4. Variations in stable transmission in relation to the temperature during heating (black dots) and cooling (red squares) of the LC sample fabricated from two non-rubbed PVK-coated glass substrates. The LC sample at 25°C; (a) before (transparent) and, (b) after (scattering) thermal treatment via the particular TIPS.

versus position curves (dotted lines) which were detected along **X** and **Y** directions, respectively. The contrast ratio of the concentric polarization rotator was measured to be 240:1.

Additionally, setting y_1 (x_1) and y_2 (x_2) to 0.1 (0.1) and 2.6 (2.8), and y_1' (x_1') and y_2' (x_2') to 3.7 (3.9) and 6.7 (6.5) in $T = T_0 \sin^2[\frac{\pi}{2}(\frac{Y(X)-y_1(x_1)}{y_2(x_2)-y_1(x_1)})]$, yields the theoretical transmittance versus position curves, as shown in Figs. 3(e) and 3(f) (solid lines), which matched the experimental results (dotted lines) closely. Such a concentric polarization rotator can be applied in a circular variable neutral density filter.

In summary, the thermally-switched LC alignments based on rubbed PVK films, and their uses in the fabrication of concentric polarization rotators were successfully demonstrated. The key to fabricating such polarization rotators is to establish a thermal gradient. The optical properties of the fabricated polarization rotators agree well with theory. The polarization rotators have potential for use as beam forming applications, density beam splitters, circular variable neutral density filters, and other applications.

3.2 Particular Thermally Induced Phase Separation of LC and PVK and Its Application [32]

The second part shows that a method of particular thermally induced phase separation (TIPS) of liquid crystals (LCs) and polymers. About the fabrication processes of LC cells, two non-rubbed PVK-coated glass substrates were combined to fabricate an empty cell, whose cell gap was 6 μm. Finally, the nematic LC (K15) was homogeneously filled into the empty cell, and the edges of the cell were sealed with epoxy to produce a sample. The fabricated LC sample was very stable at room temperature ($\sim$25°C). The details of the proposed particular TIPS are described following.

Figure 4 shows the plot of the variation in transmittance with the temperature of an LC (K15) sample fabricated from two non-rubbed PVK-coated ITO glass substrates. Experimentally, a red probed laser beam derived from a He-Ne laser ($\lambda = 632.8$ nm) was normally incident onto the temperature-controlled LC sample. The transmitted light was collected by a photo-detector placed behind the LC sample. The high transmittance remained almost unchanged when the LC sample was gradually heated (black dots) from

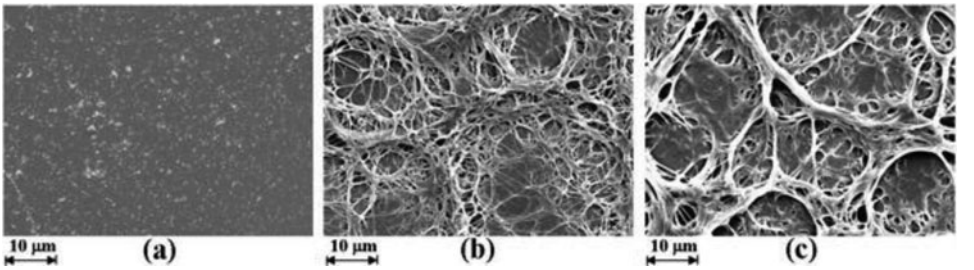

Figure 5. SEM images of LC samples after thermal treatment with setting temperatures of (a) 40, (b) 60, and (c) 80°C at a heating rate of 30°C/min. The temperature of the LC sample was maintained at the setting temperature for 8 min, and then cooled to 25°C at a cooling rate of 30°C/min.

25°C to 60°C at a heating rate of ∼5°C/min. The temperature of the LC sample was maintained at 60°C for 8 min to dissolve PVK homogeneously, which was experimentally optimized. Subsequently, the LC sample was cooled (red squares) to 25°C at a cooling rate of ∼5°C/min. The transmittance abruptly dropped at approximately 34°C during the cooling process. This point is close to the clearing temperature (∼35°C) of the used LCs (K15), given that the LC phase is transformed from isotropic to nematic at this temperature. The transparent sample became a scattering (opaque) sample after thermal treatment via the particular TIPS processes. Notably, the small variations in transmittance are caused by the temperature-dependent refractive indexes of LCs and the thermal disturbance [14, 37]. The switching temperature (T_S), which is defined as the temperature required to switch the LC sample from the transparent to the scattering mode, depends on the selected LCs. Experimentally, the T_S of the three kinds of nematic LCs, K15 (Merck), E7 (Fusol material), and MDA-00-3461 (Merck), were ∼35, ∼61, and ∼92°C, respectively. T_S was almost equal to the clearing temperatures, suggesting that the LC sample should be heated to a temperature higher than the clearing temperature and then cooled to generate disordered LC alignment. The insets (a) and (b) of Fig. 4 show the photographs of the LC sample at room temperature (∼25°C) before (transparent) and after (scattering) thermal treatment via the particular TIPS, respectively. The LC sample was heated at 60°C and then cooled at 25°C at a rate of 5°C/min. The scattering state of the thermally treated LC sample was also stable at room temperature (∼25°C). This finding indicated that the disordered LC alignment layer was permanent at temperatures below the clearing temperature of the LCs. Restated, the thermal stability of the LC light shutter can be improved by selection of LCs with proper clearing temperature. Notably, the thermal treatment conditions, such as switching temperature, for different LC materials will be different.

Three LC samples with double-sided PVK films (cell gap ∼6 μm) were heated to 40, 60, and 80°C at a heating rate of 30°C/min to investigate the effect of the setting temperature on the formation of PVK films. The setting temperature of the LC sample was maintained for 8 min to dissolve PVK homogeneously, followed by cooling to room temperature (25°C) at a rate of 30°C/min. The SEM morphologies of the LC samples after thermal treatment at the setting temperatures of 40, 60, and 80°C are shown in Figs. 5(a)–5(c), respectively. The morphologies of the rough PVK film in Fig. 5(c) are denser than those in Figs. 5(a) and 5(b). This result indicated that the roughness and amount of rough PVK increased with the setting temperature. The branch-like structures of the rough PVK film also became more prominent with a higher setting temperature, probably because the PVK solubility in isotropic LCs increases with the LC temperature. A separate

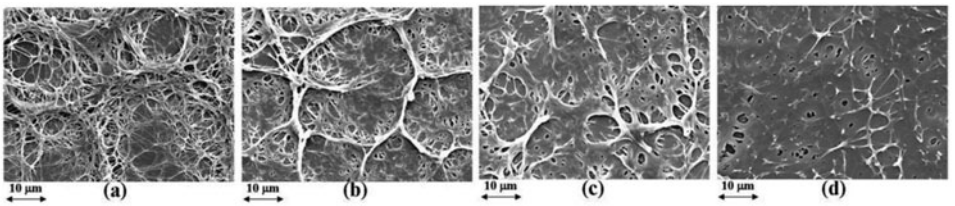

Figure 6. SEM images of LC samples after being heated to 60°C at a heating rate of 30°C/min. The temperature of the LC sample was maintained at 60°C for 8 min, and then cooled to 25°C at the cooling rates of (a) 30, (b) 10, (c) 5, and (d) 1°C/min.

experiment (data not shown) revealed that the scattering performance of the LC sample shown in Fig. 5(a) was very poor. The scattering performance of the thermally treated LC sample continuously increased and became saturated at the setting temperature of ∼60°C with higher setting temperature. Optically, the measured transmittances of the LC samples in Figs. 5(b) and 5(c) were identical. These findings indicated that the setting temperature of thermal treatment is the key in the fabrication of the scattering mode LC light shutter.

Four fabricated LC samples with double-sided PVK films (cell gap = ∼6 μm) were heated to 60°C at a heating rate of 30°C/min to study the effect of the cooling rate on PVK film formation. The temperatures of the LC samples were maintained at 60°C for 8 min to dissolve PVK homogeneously, and then cooled to room temperature (25°C) at cooling the rates of 30, 10, 5, and 1°C/min [Figs. 6(a)–6(d)]. The SEM images revealed that the dimension and roughness of the branch-like structures increased with increasing cooling rate. The scattering performance of the LC samples directly increased with the cooling rate. In a previous study [38], the surface morphology of polymers fabricated via TIPS at a slow cooling rate is more uniform and regular than those at a fast cooling rate. A rougher PVK structure is associated with higher scattering. The effect of the cooling rate in TIPS is similar to that of the light intensity in PIPS by illumination. Moreover, a separate experiment (data not shown) shows that the scattering capability decreases with the increase of the cell gap. Experimentally, the processes and conditions of the thermal treatment were identical to those used in Fig. 5, except that the cell gaps varied and the cooling rate was fixed at 30°C/min. The distribution of the LCs in the bulk of the large-cell-gap LC sample after thermal treatment was more difficult to disturb and tended to preserve its original alignment, thus leading to large LC domains. The driving voltage also increased with increased cell gap, resulting in the reduced performance of the LC light shutter.

Figure 7 shows the plots of the measured transmittance of the scattering mode LC light shutter [fabricated under treatment conditions consistent with those in the insets (a) and (b) of Fig. 4] as a function of an applied alternating current (AC; 1 KHz) voltage. Transmittance was defined as the ratio of the intensity of the transmitted beam through the thermally treated LC sample to that through an empty cell, such that the transmission through an empty cell was equivalent to 100%. The required voltage to achieve maximum transmittance (∼76.7%) was about 18 V. A low applied AC voltage of ∼13 V was required to switch the LC light shutter from the scattering mode to 90% of its maximum transmittance. Notably, the small cell gap and the weak surface anchoring resulting from the rough PVK layers are the keys to reduce the driving voltage. Additionally, the operated voltage, which was inversely proportional to the square root of the dielectric anisotropy ($\Delta\varepsilon$), can be reduced to a greater extent using LCs with higher $\Delta\varepsilon$ values. The contrast ratio, defined as the maximum transmittance ($V = \sim 18$ V) over the minimum transmittance ($V = 0$ V),

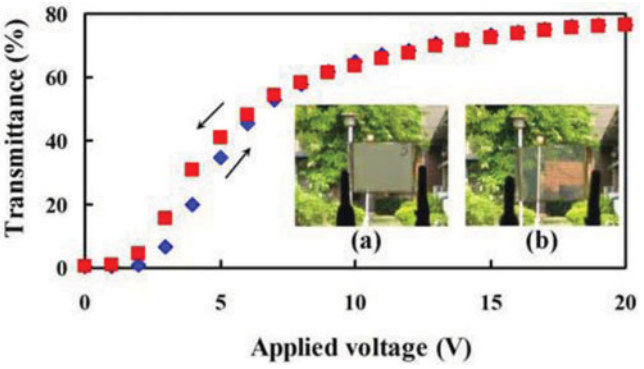

Figure 7. Measured transmission of the fabricated scattering mode LC light shutter as a function of an applied AC (1 KHz) voltage. Insets show photographs of the LC light shutter at 25°C with the applied AC voltages of (a) 0 and (b) 18 V.

of the light shutter was calculated to be 300:1. Photographs of the LC light shutter at 25°C with applied AC voltages of 0 and 18 V are shown in the insets (a) and (b) of Fig. 7, respectively. Moreover, the LC ($\Delta\varepsilon > 0$) domains became aligned along the electric field as an AC voltage was applied, leading to a reduction in the refractive index mismatch (volume scattering). Thus, the scattering mode LC light shutter can be electrically switched from the opaque to the transparent mode. Notably, the transmittance cannot reach 100% considering that the fog-like scattering (surface scattering) was caused by the refractive index mismatch between n_o of the selective LCs and $n_{PVK.}$ Accordingly, proper selection of the used LCs with n_o equivalent to n_{PVK} can enhance transmittance. Theoretically, the surface scattering, resulting from the refractive index mismatch between n_{eff} (1.53 $\sim$ 1.7) of the LCs and n_{PVK} (1.68), should be increased with the applied voltage. According to the transmittance of the light shutter with applied AC voltages of 0 and 20 V, shown in Fig. 7, the volume scattering provides the main contribution to demonstrate the electrically switchable LC light shutter.

Figure 8 shows the dynamic response of the fabricated scattering mode LC light shutter when an AC voltage pulse is applied. The amplitude and the frequency of the pulse are 20 V and 1 KHz, respectively. The measured rise and fall times refer to the period required to change the transmittance of the light shutter from 10% to 90% and from 90% to 10% of

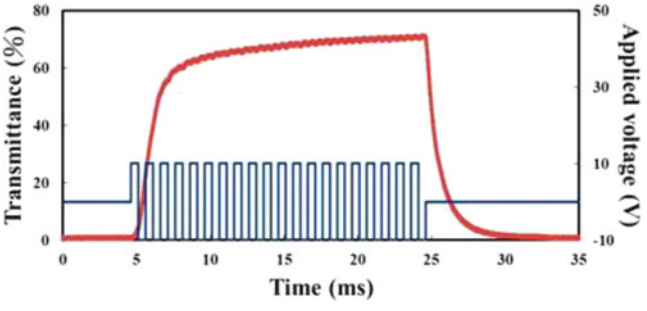

Figure 8. Dynamic response (red line, plotted on the primary axis) of fabricated scattering mode LC light shutter when an AC voltage pulse (blue line, plotted on the secondary axis) of 20 V (1 KHz) is applied.

its maximum transmittance, respectively. The rise and fall times for the scattering mode LC light shutter were about 2.25 and 3.22 ms, respectively. Notably, the backflow effect, which increases the response time, is not observed in Fig. 8. Moreover, the inner PVK structures of the LC light shutter provide a weak surface anchoring to result in the fast orientation of LC molecules, i.e. fast response [14]. However, the electrically induced carrier injection from ITO/PVK into LC should be considered because PVK is well known photo-conducting polymers for UV spectral region. According to Refs. 39 and 40, DC field and applied voltage with low frequency but not the applied voltage with high frequency, may result in the accumulation of charge carriers inside the LC bulk, which will reduce the performance of the LC light shutter severely. In case of reduction of performance, anti-UV coatings onto the substrates can be adopted to eliminate the carrier injection, produced by PVK.

In summary, a particular TIPS method of LCs and polymers was presented. The method was used in the successful fabrication of a scattering mode LC light shutter from LC samples consisting of double-side PVK films. Permanent scattering resulted from the formation of multiple and micron-sized domains of disordered LCs. The fabricated LC light shutter possessed the advantages of low driving voltage, fast response in the order of milliseconds, independent of polarization, high contrast ratio (∼300:1), and being polarizer free. The effects of different switching temperatures, cooling rates, and cell gaps on the formation of LC light shutter were also investigated. Moreover, the electrically switchable LC light shutter in the scattering mode had extremely promising potential applications, such as in energy-efficient smart windows and scattering mode LC displays.

3.3 Optically and Thermally Controllable Light Scattering and Its Application [41]

The final part presents the optically controllable light scattering based on dye-doped liquid crystals (DDLCs) in a cell, whose substrates are coated with PVK films. The optical control mechanism is the light-induced dissolution of PVK in DDLCs, which reforms the disordered LC distribution into multiple and micron-sized LC domains. The induced thermal effect on the process is investigated in detail. Scanning electron microscopy images are obtained to show the surface structures of the produced PVK films. The generated scattering can be switched back to the original one by particular thermally induced phase separation. Results indicate that the light-induced thermal effect and photoisomerization lead to the dissolution of PVK in DDLCs. Finally, scattering mode light shutter with different transmission is successfully achieved by illuminating the cell under various light intensities.

Two non-rubbed PVK-coated glass substrates were combined to fabricate an empty cell with a cell gap of 6 μm. The azo dye, DR1, was doped into the LC host at a concentration of ∼1.5 wt%. The DR1-doped LC was homogeneously filled into the empty cell, and the edges of the cell were then sealed with epoxy to yield the cell. According to our previous work, the transparent cell will become scattering (become opaque) one after thermal treatment via particular TIPS processes [32]. High scattering can provide an efficient dark state that can be used to fabricate light-modulation devices. Thus, the originally fabricated cell was treated with a particular TIPS process. Finally, the high-transmittance cell was gradually heated from 25°C to 80°C at a heating rate of ∼30°C/min. The DDLCs cell temperature was maintained at 80°C for 5 min to dissolve PVK homogeneously. Subsequently, the DDLCs cell was cooled to 25°C at a cooling rate of ∼30°C/min. The transmittance abruptly dropped to 0.4% at approximately 54°C during cooling.

Figure 9(a) shows the experiment setup for the optically switched scattering state in this system. A diode-pumped solid-state (DPSS) laser ($\lambda = 532$ nm) was used to illuminate the scattering DDLCs cell. To produce a light beam with a uniform intensity, the laser beam

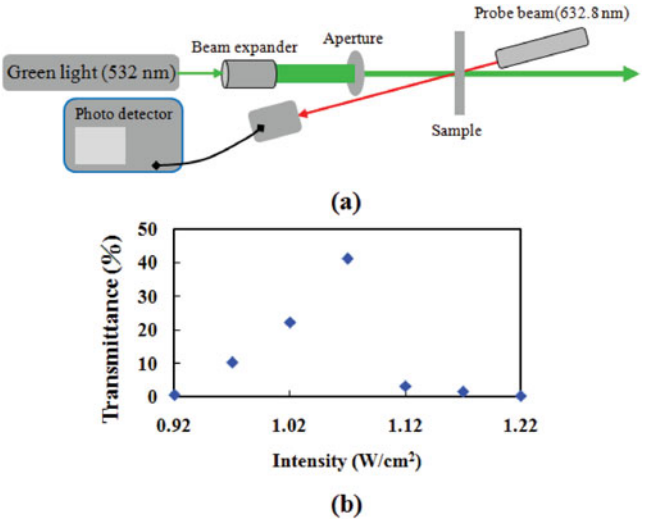

Figure 9. (a) Experiment setup for the optical modulation of the scattering performance. The diameter of the illuminated spot is ∼3 mm. (b) Transmittances of the stable scattering modes, which were achieved under different green light intensities. The probed beam is a He-Ne laser beam.

from the laser head was passed through an expander and an aperture, and finally illuminated onto the DDLCs cell. The diameter of the illuminated spot is approximately 3 mm. The duration of the illumination is 10 min, and the selected intensities of green light are 0.92, 0.97, 1.02, 1.07, 1.12, 1.17, and 1.22 W/cm^2. Notably, after we obtained one transmission of the stable scattering, the DDLC cell was then treated with particular TIPS to switch the transmission back to the original scattering state (original PVK morphology) before another intensity green light was illuminated onto the DDLC cell. To monitor the scattering performances, a red probe beam from an unpolarized He-Ne laser ($\lambda = 632.8$ nm) was normally incident onto the illuminated spot of the DDLCs cell. The transmitted red light was received by a photodetector placed behind the DDLCs cell. The various transmittances of the stable scattering modes probed by the He-Ne laser were obtained under different green light intensities [Fig. 9(b)]. Therefore, the transmittance depends on the green light intensity. Notably, 100% transmittance was defined as the transmittance of the transparent cell after being filled with DDLCs without thermal treatment (particular TIPS processes). Experimentally, the stable transmittance was optically modulated ranging from 0.1% and 41.2%. The optically and thermally controllable scattering mode light shutter with different transmission is produced. The green light illumination process can modulate the original scattering state to other scattering one with transmission of 0.1%–41.2%. The transmission of the optically controllable scattering mode light shutter after blocking the green light is stable. Accordingly, the multistable scattering LC light shutter is demonstrated. The minimum transmittance (0.1%) of the optically reproduced DDLCs cell is lower than that of a scattering DDLCs cell after thermal treatment via particular TIPS processes [32]. The reason for this mechanism is discussed in later sections.

The following experiments were conducted to verify the mechanism of the light-induced dissolution of PVK into DDLCs for the modification of the scattering performance of DDLCs cells. These experiments were performed to study the light-induced thermal effect, which plays a key role in the process of scattering modulation. In brief, a thermal

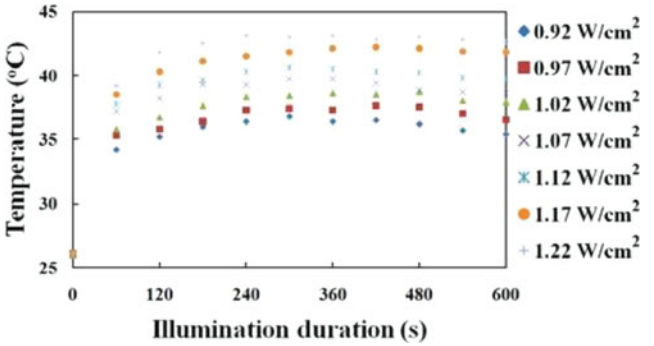

Figure 10. Temperature variations as a function of the duration of green light illumination onto the scattering DDLCs cell. The cell was fabricated using two non-rubbing PVK-coated glass substrates after thermal treatment via particular TIPS processes.

imager (IRI 4040, Irisys) was used to measure the DDLCs cell temperature under green light illumination. Figure 10 shows the temperature variations as a function of the duration of green light illumination onto the scattering DDLCs cell. Initially, the clearing temperature of the DDLCs sample was approximately 54°C. The experimental results show that the temperature of the scattering DDLCs sample rapidly exceeded 34°C under green light illumination for approximately 60 s. A higher green light intensity can exert a stronger light-induced thermal effect on the DDLCs cell. Moreover, the DDLCs cell temperature slightly decreased after 300 s. The reasons for this finding are as follows: first, the scattering performance decreases with increasing duration of green light illumination. Therefore, the reduction in light-scattering mean free path results in temperature reduction after 300 s [42]. Second, as described above, DR1 dye is a kind of dichroic dyes; the molecular reorientation of the DR1 molecules induced by the photoisomerization process leads to an anisotropic absorption of light [43–45]. Thus, the absorbance of the polarized green light by the DDLCs is reduced, so that its temperature slightly decreases. Thirdly, the adsorption of 532 nm light by *cis* isomers is lower than that by *trans* isomers [46]. Accordingly, the absorption of green light decreases, resulting in slight reduction of temperature. After that, the green light is turned off after 600 s, and the DDLC temperature will decrease to room temperature naturally. The cooling time is about 40 s, depending on the green light intensity. Therefore, the increase and recovery time of the multistable scattering LC light shutter are about 640 s and 300s, respectively. The switching time can be improved by properly selected LCs, azo materials, green light intensity and others.

Based on our previous study [32], the coated PVK can be dissolved into the LCs after heating under temperatures higher than the switching temperature (T_S). T_S is defined as the temperature needed to change the mode of the LC cell from transparent to scattering. Moreover, T_S depends on the selected LCs. The separate experiments reveal that the T_S obtained without green light illumination is approximately 54°C, which is close to the clearing temperature of the selected LCs. Thus, the solubility of PVK in DDLCs can be enhanced because of the low-order parameter of the photoisomerized *cis*-isomers in the DDLCs cell, and T_s is reduced to approximately ∼35°C. In addition, the structures of the PVK that reformed on the substrates and were fabricated via different dissolution processes were observed using scanning electron microscopy (SEM). The SEM images are shown below.

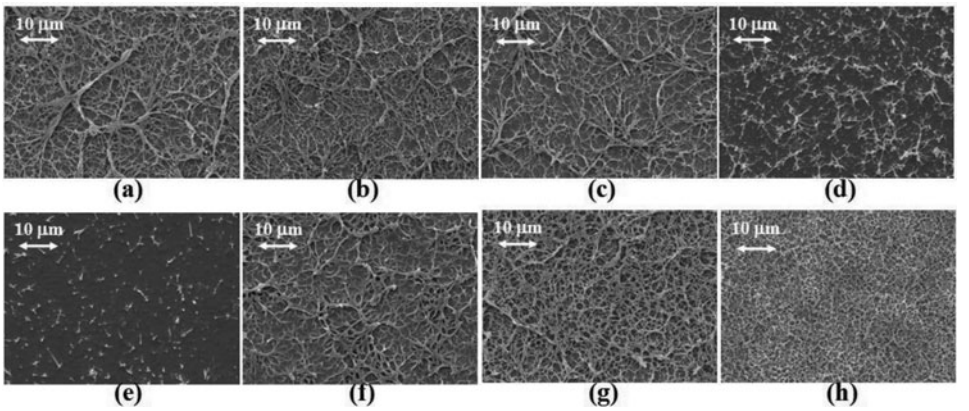

Figure 11. SEM images of DDLCs cells before and after treatment with light-induced PVK dissolution based on DDLCs scattering as a result of particular TIPS processes: (a) morphologies of the initial thermally treated PVK film (no light illumination). The intensities of the green light irradiated onto the scattering DDLCs cell are (b) 0.92, (c) 0.97, (d) 1.02, (e) 1.07, (f) 1.12, (g) 1.17, and (h) 1.22 W/cm^2.

Figure 11 shows the SEM images of the DDLCs cell substrates before and after treatment with light-induced PVK dissolution. The intensities of the green light irradiated onto the scattering DDLCs cell are 0.92, 0.97, 1.02, 1.07, 1.12, 1.17, and 1.22 W/cm^2. The SEM images reveal that the dimensions and roughness of the branch-like structures are determined by the different green light intensities. The initial thermally treated PVK structures are shown in Fig. 11(a). Figures 11(b)–11(e) show that the original branch-like PVK structures were dissolved by DDLCs under illumination of green light with intensities of 0.92, 0.97, 1.02, and 1.07 W/cm^2, respectively. The phase separation of the dissolved PVK and DDLCs occurred after switching off the green light, which facilitated the reformation of the PVK surfaces. Under these four intensities, the surfaces of the reformed PVK structures became increasingly more uniform and smoother as the green light intensity increased. In other words, the branch-like PVK morphologies were destroyed. Thus, the transmission of the DDLCs cell increased with increasing green light intensity (at intensities below 1.07 W/cm^2). This finding indicates that the solubility of PVK in these four cases remains low, and that only the branch structures of PVK on substrates close to the bulk can be dissolved by DDLCs under green light illumination. Moreover, the *cis*-isomers in these four cases are too few to sufficiently reduce the order parameter (clearing temperature) of the DDLCs because of the low green light intensity. The phase separation rates in Figs. 11(b)-11(e) should therefore be low. In consideration of this point as well as the amount of dissolved PVK, the surfaces of the slowly produced, reformed PVK tend to be uniform [Figs. 11(b)–11(e)]. In other words, the few dissolved PVK molecules in DDLCs cannot sufficiently reform the rough surface structures to provide high scattering after green light blocking. Figures 11(f)–11(h) show the SEM images of the DDLCs cell substrates after treatment with green light illumination at 1.12, 1.17, and 1.22 W/cm^2 intensities, respectively. Figure 9(b) shows that all three DDLCs cells exhibit high scattering performances. Moreover, the reformed PVK are mesh-like structures whose density increased as the green light intensity increased. Briefly, experimentally, when the illumination green light exceeds 1.12 W/cm^2, the solubility of the PVK film by DDLCs is high enough to dissolve not only the branch structures of PVK on substrates close to the bulk

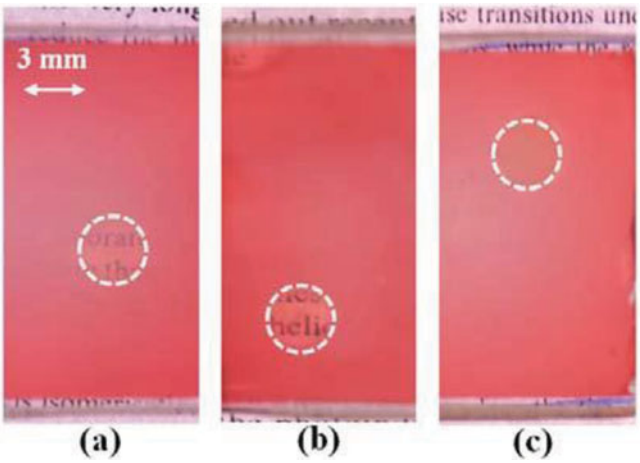

Figure 12. Images of the optically controllable multistable light shutter based on the DDLCs sample. The intensities of the green light are (a) 0.97, (b) 1.07, and (c) 1.22 W/cm^2. The areas marked by the white dotted lines are the illuminated areas with diameters of ∼3 mm.

but also the PVK film close to substrate. After switching off the green light, phase separation occurs, and mesh-like structures are reproduced. In our previous study [32], the cooling rates (phase separation rates) of the particular TIPS processes determine the surface roughness of the PVK structures. A rougher PVK structure is associated with higher scattering. A comparison of Figs. 11(e) to 11(h) reveals that the solubility significantly increased under green light illumination at intensities above 1.12 W/cm^2. This finding indicates that the solubilities of PVK in DDLCs significantly increased. The solubility of PVK in isotropic LC is higher than that in nematic LC [32]. Thus, the *cis*-isomers of the azo dye clearly lowered the clearing temperature of the DDLCs, which resulted in the increased solubility shown in Figs. 11(f)–11(h).

Figure 12 shows the images of the optically controllable scattering light shutter based on the DDLCs cell. The green light intensities are 0.97, 1.07, and 1.22 W/cm^2, and the corresponding transmittances of the DDLCs cell are 10.2%, 41.2%, and 0.1%, respectively. The diameter of the illuminated area is approximately 3 mm. The illuminated areas represent variable scattering performances, which are determined by the different sizes of the LC domains. The scattering performance can be easily modulated by green light illumination at different intensities. Moreover, the transmittance/scattering of the optically controllable DDLCs light shutter can be completely switched back to the original scattering state via treatment with the particular TIPS.

In summary, a multistable, scattering-mode, LC light shutter was presented in this study. The scattering performances resulting from the multidomains of disordered LCs can be easily controlled by green light illumination. In brief, PVK dissolution into DDLCs and phase separation are the keys to the generation of optically controllable scattering light shutter. Moreover, heating by light-induced thermal effect and the reduction of the DDLCs clearing temperature (isothermal phase transition) are the major effects of PVK dissolution, which result in optically and thermally controllable light scattering. In addition, the advantages of the reported light scattering shutter include the reduction in power consumption, multistability, optical control, and others. The optically controllable and

multistable light scattering shutter can be used in several LC applications, such as energy-efficient smart windows, scattering mode LC displays, and others.

4. Conclusion

This paper demonstrates the alignment properties of LCs and a novel phase separation method using PVK layers as alignment films. Several LC devices have also been developed and fabricated using the PVK properties, including the alignment, the dissolution of PVK and LCs, and light-induced scattering modulation. All of them can be read in this paper. We believe that PVK is a potential material for fabricating LC devices. These fabrications of the devices are simple, highly reliable, and convenience to use. The electro-optical properties of PVK have not yet studied completely. Thus, the continuous investigation of PVK has highly scientific values.

Acknowledgments

The authors would like to thank the National Science Council (NSC) of Taiwan for financially supporting this research under Grant Nos. NSC 101-2112-M-006-011-MY3 and NSC 99-2112-M-008-021-MY3. This work is also partly supported by the Advanced Optoelectronic Technology Center.

References

[1] Yang, D. K., Chien, L. C., & Doane, J. W. (1992). *Appl. Phys. Lett.*, *60*, 3102.
[2] Bao, R., Liu, C. M., & Yang, D. K. (2009). *Appl. Phys. Express*, *2*, 112401.
[3] Ren, H., & Wu, S. T. (2002). *J. Appl. Phys.*, *92*, 797.
[4] Nersisyan, S., Tabiryan, N., Steeves, D. M., & Kimball, B. R. (2009). *Opt. Express*, *17*, 11926.
[5] Fuh, A. Y. G., Chiang, J. T., Chien, Y. S., Chang, C. J., & Lin, H. C. (2012). *Appl. Phys. Express*, 5, 072503.
[6] Cheng, K. T., Liu, C. K., Ting, C. L., & Fuh, A. Y. G. (2007). *Opt. Express*, *15*, 14078.
[7] Sinclair, G., Jordan, P., Courtial, J., Padgett, M., Cooper, J., & Laczik, Z. J. (2004).*Opt. Express*, *12*, 5475.
[8] Chapin, S. C., Germain, V., & Dufresne, E. R. (2006). *Opt. Express*, *14*, 13095.
[9] Ren, H., & Wu, S. T. (2010). *Appl. Phys. Lett.*, *90*, 121123.
[10] Huang, C. Y., Tsai, H. Y., Wang, Y. H., Huang, C. M., Lo, K. Y., & Lee, C. R. (2010). *Appl. Phys. Lett.*, *96*, 191103.
[11] Doane, J. W., Vaz, N. A., Wu, B. G.. & Zumer, S. (1986). *Appl. Phys. Lett.*, *48*, 269.
[12] Fuh, A. Y. G., & Caporaletti, O. (1989). *J. Appl. Phys.*, *66*, 5278.
[13] Lin, Y. H., Ren, H., & Wu, S. T. (2004). *Appl. Phys. Lett.*, *84*, 4083.
[14] Wu S. T. *et al.* (2001). *Reflective Liquid Crystal Displays*, Wiley: New York, USA.
[15] Fuh, A. Y. G., Chen, C. C., Liu, C. K., & Cheng, K. T. (2009). *Opt. Express*, *17*, 7088.
[16] Huang, C. Y., Ma, J. M., Mo, T. S., Lo, K. Y., Huang, S. Y., & Lee, C. R. (2009). *Opt. Express*, *17*, 22386.
[17] Huang, S. Y., Wung, T. C., Fuh, A. Y. G., Yeh, H. C., Huang, C. Y., Ma, C. M., Huang, S. C., Mo, T. S., & Lee, C. R. (2009). *Appl Phys B.*, *97*, 749.
[18] Golemme, A., Kippelen, B., & Peyghambarian, N. (1998). *Appl. Phys. Lett.*, *73*, 2408.
[19] Chen, Y. D., Fuh, A. Y. G., Liu, C. K., & Cheng, K. T. (2011). *J. Phys. D-Appl. Phys.*, *44*, 215304.
[20] Chen, Y. D., Cheng, K. T., Liu, C. K., & Fuh, A. Y. G. (2011). *Opt. Express*, *19*, 7553.
[21] Kaczmarek, M., & Dyadyusha, A. (2003). *J. Nonlinear Opt. Phys. Mater.*, *12*, 547.
[22] Hasegawa, M. (2000). *Jpn. J. Appl. Phys.*, *39*, 1272.

[23] Nakajima, K., Wakemoto, H., Sato, S., Yokotani, F., Ishihara, S., & Matsuo, Y. (1990). *Mol. Cryst. Liq. Cryst.*, *180*, 223.
[24] Amra, C. (1993). *Appl. Opt.*, *32*, 5481.
[25] Duparre, A., & Kassam, S. (1993). *Appl. Opt.*, *32*, 5475.
[26] Dierking, L. L., Kosbar, A. A., Ardakani A. C., Lowe, & Held, G. A. (1997). *J. Appl. Phys.*, *81*, 3007.
[27] Kim, I. I., McArthur, B., & Korevaar, E. (2001). *Proc. SPIE*, *4214*, 26.
[28] Wong, W. Y. Y., Wong, T. M., & Hiraoka, H. (1997). *Appl. Phys. A*, *65*, 519.
[29] Hervet, H., Urbach, W., & Rondelez, F. (1979). *J. Chem. Phys.*, *68*, 2725–2729.
[30] Galstyan, T. V., Drnoyan, V. E., & Arakelian, S. M. (1996). *Phys. Lett. A*, *217*, 52.
[31] Chen, A. G., & Brady, D. J. (1992). *Opt. Lett.*, *17*, 441.
[32] Chen, Y. D., Fuh, A. Y. G., & Cheng, K. T. (2012). *Opt. Express*, *20*, 16777.
[33] Freedericksz, V., & Zolina, V. (2013). *Trans. Faraday Soc.*, *29*, 919.
[34] Ren, H., Fan, Y.-H., Gauza, S., & Wu, S. T. (2004). *Appl. Phys. Lett.*, *84*, 4789.
[35] Fuh, A. Y. G., Ko, S. W., Huang, S. H., Chen, Y. Y., & Lin, T. H. (2011). *Opt. Express*, *19*, 2294.
[36] Fuh, A. Y. G., Chen, J. C., Cheng, K. T., & Huang, S. Y. (2010). *J. Soc. Inf. Disp.*, *18*, 572.
[37] Li, J., Gauza, S., & Wu, S. T. (2004). *J. Appl. Phys.*, *66*, 19.
[38] Jin, J. M., Parbhakar, K., & Dao, L. H. (1996). *Langmuir*, *12*, 2096.
[39] Song, L., Lee, W. K., & Wang, X. (2006). *Opt. Express*, *14*, 2197.
[40] Sun, X., Pei, Y., Yao, F., Zhang, J., & Hou, C. (2007). *J. Phys. D-Appl. Phys.*, *40*, 3348.
[41] Chen, Y. D., Fuh, A. Y. G., & Cheng, K. T. (2012). *Opt. Express*, *20*, 26252.
[42] García, P. D., Sapienza, R., Froufe-Pérez, L. S., & López, C. (2009). *Phys. Rev. B*, *79*, 241109.
[43] Gorkhali, S. P., Cloutier, S. G., Crawford, G. P., & Pelcovits, R. A. (2006). *Appl. Phys. Lett.*, *88*, 251113.
[44] Namdar & Tajalli, H. (2004). *Laser Phys.*, *14*, 1520.
[45] Materny, B. A., Steins, H., Müller, M. M., & Schottner, G. (1998). *Macromolecules*, *31*, 4265.
[46] Fuh, A. Y. G., Lin, H. C., Mo, T. S., & Chen, C. H. (2005). *Opt. Express*, *13*, 10634.